PHILOSOPHICAL TRANSACTIONS OF THE ROYAL SOCIETY A MATHEMATICAL, PHYSICAL & ENGINEERING SCIENCES

Chromosphere and Corona: Observations of the Extreme Ultraviolet Solar Spectrum

R. Tousey

Phil. Trans. R. Soc. Lond. A 1971 **270**, 59-70
doi: 10.1098/rsta.1971.0060

Phil. Trans. Roy. Soc. Lond. A. **270**, 59–70 (1971) [59]
Printed in Great Britain

II. CHROMOSPHERE AND CORONA

Observations of the extreme ultraviolet solar spectrum

By R. Tousey
E. O. Hulburt Center for Space Research, U.S. Naval Research Laboratory, Washington, D.C. 20390, *U.S.A.*

[Plates 4 to 7]

The present state of knowledge of the Sun's extreme ultraviolet spectrum is reviewed, and areas for future work are indicated. Recent extreme ultraviolet spectroheliograms, including one that shows an importance 2*N* flare, are discussed.

Introduction

In the twenty-four years since the first observation of the Sun's ultraviolet spectrum beyond the limit set by the Earth's atmosphere, so much has been learned about its extreme ultraviolet radiating characteristics that a review, if short, must be far from complete. I shall simply summarize the current status of extreme u.v. observations carried out from space vehicles, and indicate some of the work to be done in the future. The spectral range will be limited to 208.5 to 1.5 nm†; this includes the radiation emitted by the temperature minimum, chromosphere, and corona. The range will be discussed by sections, chosen on the basis of available observing techniques and the nature of the spectrum itself. In the last part, some of the best extreme u.v. spectroheliograms are reproduced, including one that shows the spectrum and form of a flare.

Normal-incidence spectroscopy

The region 208.5 to 91.2 nm is receiving a great deal of attention because it covers the range where the last vestiges of the photosphere disappear and the spectrum changes to one that is really chromospheric and coronal. About 700 emission lines have been listed, and of the order of half have been identified. The section 153 to 170 nm is of particular interest because it includes the greatest mixture of radiations from different regions. Three spectra for a 15 nm span centred near 166 nm are reproduced in figure 1, plate 4. They illustrate the confused nature of the spectrum and the change in character with height above the limb. At the bottom is a spectrum having 20 pm† resolution, made by N.R.L. when the Sun was quiet (Tousey *et al.* 1964). Because this spectrum is stigmatic, the ends of the lines show the change of intensity with altitude at opposite positions on the limb; the spatial resolution is approximately 10″. Chromospheric lines can be distinguished by their limb brightening, for example, He II, 164.047 nm. In the centre is the Culham spectrum of 9 April 1965 (Burton, Ridgeley & Wilson 1967), made with the slit positioned 10″ above the limb, hence the lines are mostly chromospheric to inner coronal. These lines match the very ends of corresponding lines in the stigmatic spectrum, and permit determining chromospheric intensities with greater accuracy than can be done from line-ends. The off-limb spectrum is also of great assistance in confirming in the N.R.L. spectrum the classification of lines as chromospheric, coronal, or temperature minimum, and in deciding which lines within

† 1 nm = 1000 pm = 10Å.

confused regions are really emission lines and which are simply continuum exposed to view between Fraunhofer lines.

The top spectrum is a short section of the flash spectrum obtained by N.R.L. during the total eclipse of 7 March 1970 (Brueckner, Bartoe, Nicolas & Tousey 1970). During this eclipse, photographic extreme u.v. spectrographs basically similar in design were flown into the total eclipse shadow in two Aerobee rockets which were launched from Wallops Island, Virginia, the one immediately after the other. The second vehicle carried instruments prepared by a consortium comprised of the Imperial College of London, the Culham Laboratory, the University of York, Toronto, and the Harvard College Observatory. Results from the latter flight are reported in another paper (Speer *et al.* 1970). The parachute recovery systems for the two payloads were identical, but N.R.L.'s failed for cause unknown. An instant after plunging into the sea the evacuated and watertight instrument section imploded with great violence, then sank gradually and came to rest on the bottom at a depth of about 1800 m. However, an operation directed by the Supervisor of Salvage of the U.S. Navy succeeded in locating and retrieving the payload on 22 March 1970.

The eclipse spectra had been photographed on Eastman Kodak Film 101–01, a Schumann-type emulsion containing almost no gelatine, with the silver halide grains completely unprotected. The exposed film had been immersed for fifteen days in sea water at a pressure of about 20 MN m^{-2} (200 atm) and at a temperature of 5 °C. Surprisingly, laboratory tests indicated that under these conditions the latent images should have survived. However, intense electrolytic action took place within three of the metal cameras and the images were ruined by the chemical products involved. The film strips within the fourth camera, covering 140 to 196.5 nm, escaped total loss because the inside of this camera had been spray-coated with Teflon. The section reproduced in figure 1 was from a 5 s exposure that took place just before second contact, with the central part of the crescent changing width from 4.5 to 2.2″ of photosphere. One end of the crescent has been masked off, to secure a match to the other spectra. The central portion includes radiation from the outermost part of the photosphere, the chromosphere, and the corona, but the ends of the long crescents are from the chromosphere and corona only.

It is obvious that this flash spectrum suffered greatly from the chemical environment and is suitable for only the crudest kind of photometry. However, the spectral resolution was not greatly degraded and much can be learned from the crescent lengths. All six lines of C I, $2p^2\,{}^3P–3s\,{}^3P^0$ near 165.7 nm are resolved, in the original even the two that are separated by 12 pm. Conspicuous because of its great extension into the chromosphere is He II, 164.0474 nm.

Extreme ultraviolet flash spectra will be of the greatest value in line identification, and for deriving the best model of the solar atmosphere from the temperature minimum up through the chromosphere and into the corona. But in addition to eclipse spectra, increased resolution is needed to untangle completely the region 208.5 to 91.2 nm. A start in this direction has been made by the Harvard College Observatory using a photoelectric scanning spectrometer covering the range 140 to 187.5 nm with about 7 pm resolution (Parkinson & Reeves 1969).

Increased resolution is also required to locate the level of the continuum whose absolute value in this region is extremely important in connexion with the value of the minimum solar temperature. At present, the results are in conflict; N.R.L.'s minimum temperature for the continuum is about 4670 K (Sandlin & Widing 1967; Widing, Purcell & Sandlin 1970) and Harvard's is 4400 K (Parkinson & Reeves 1969). The difficulty of distinguishing the continuum is evident from figure 1, where the last clearly distinguished and identified Fraunhofer line is Si I, 169.33 nm,

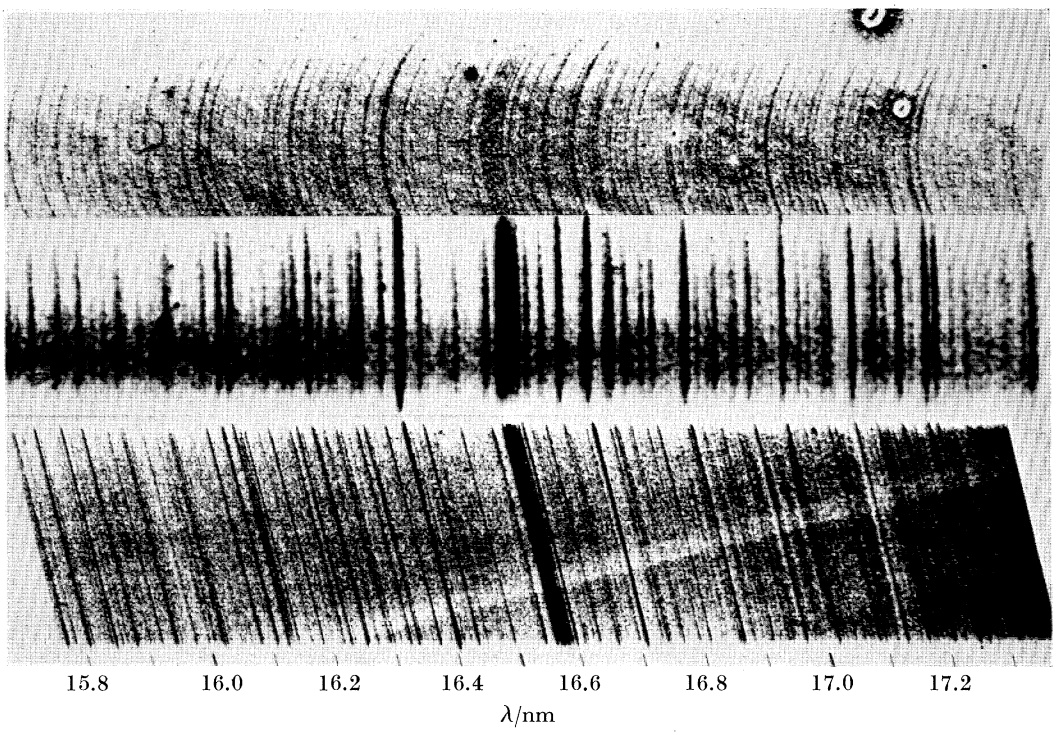

FIGURE 1. Solar spectra over a range that includes radiation from the temperature minimum and the chromosphere, with some contribution from the photosphere and the inner corona. At the top is a total eclipse flash spectrum obtained on 7 March 1970 by N.R.L. In the centre is the Culham 10″ off-limb spectrum of 9 April 1965. The bottom shows the N.R.L. double-dispersion spectrum of 1 February 1966, having a spatial resolution of about 10″.

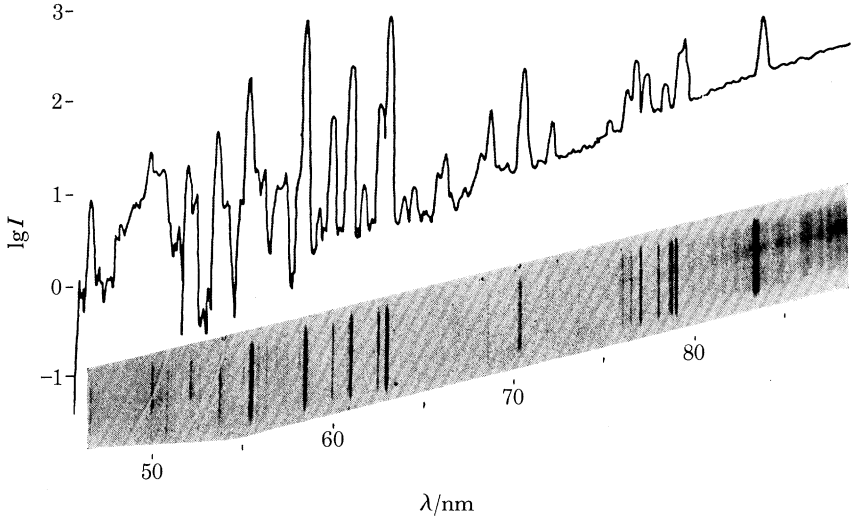

FIGURE 2. The N.R.L. double-dispersion stigmatic spectrum made on 27 July 1966 when the Sun was active, and an OSO–IV spectral scan of a 1′ × 1′ region at the centre of the disk, recorded by the Harvard College Observatory.

(*Facing p.* 60)

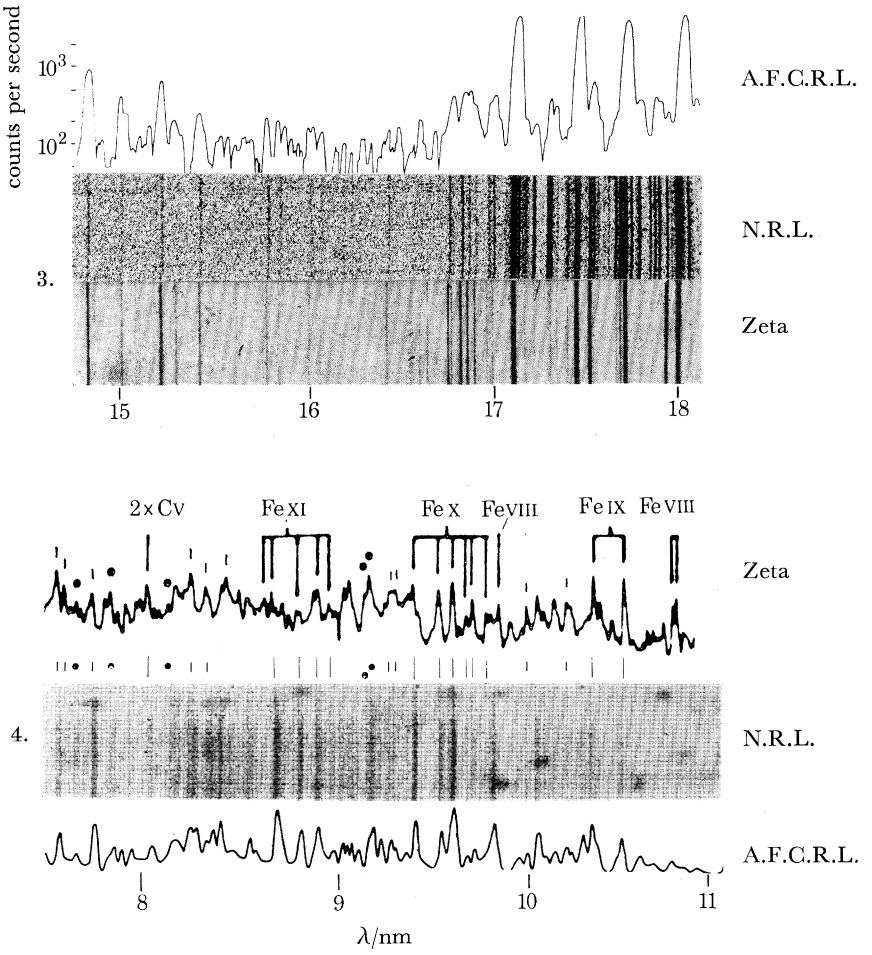

FIGURE 3. The N.R.L. spectrum of 20 September 1963 matched to the A.F.C.R.L. spectrum of 2 May 1963 and the spectrum obtained by the Culham Laboratory from the high temperature plasma produced by the Zeta discharge at Harwell.

FIGURE 4. The Sun's soft X-ray spectrum; photographed by N.R.L., scanned photoelectrically by A.F.C.R.L., and matched to a microphotometer trace of a photographic spectrum of the Zeta discharge, made by the Culham Laboratory.

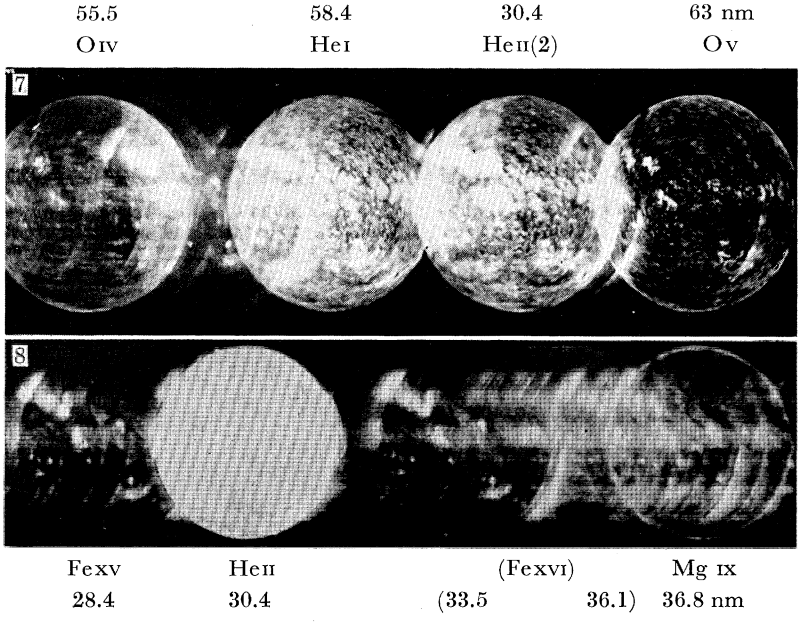

FIGURE 7. A spectroheliogram made by N.R.L. on 22 September 1968 with a 3600 line/mm 1 m radius objective-type grating spectrograph. The principal images are from the indicated chromospheric lines. Also easily seen are FeXV, 28.4 nm in second order, and MgX, 61, 62.5 nm.

FIGURE 8. A long exposure spectroheliogram made by N.R.L. on 22 September 1968 using a 3600 line/mm, 1 m radius objective-type grating spectrograph. The SiXI, 30.331 nm image is resolved from the HeII, 30.378 nm image. A great prominence is present in HeII on the right, extending above the centre line.

and the smooth sections usually contain faint, blended lines. The origin of continuum in the off-limb spectrum is unclear, whether it is photospheric stray light or true chromospheric radiation, or both. Eclipse spectra should provide a solution.

Of the future instruments for observing this spectral range, perhaps the most powerful is the large, double-dispersion spectrograph now under construction by N.R.L. for flight in the Apollo telescope mounting (A.T.M.) of Skylab I. This instrument is designed to have 8 pm spectral resolution, 2″ spatial resolution normal to the 1′ long slit, and the capability of photographing spectra of any selected solar feature.

The region below the Lyman limit, 91.2 nm, is difficult to record with normal-incidence instruments because of the low reflectance of mirrors and gratings. Nevertheless, excellent results have been obtained. There is shown in figure 2 a photographic, stigmatic, double-dispersion spectrum obtained by N.R.L. during quiet solar conditions with the slit lying across a solar diameter (R. Tousey *et al.* unpublished); this is matched against a photoelectrically scanned spectrum recorded by the Harvard College Observatory normal-incidence monochromator in OSO–IV, which received radiation from a 1′ × 1′ area at the centre of the disk (Goldberg *et al.* 1968).

From 91.2 to 63.5 nm only about twenty-five lines have been distinguished, but most of them have been identified. The Lyman continuum of hydrogen is prominent, and obscures all but the strongest lines unless the slit is narrow. The photographic spectrum of figure 2, made with a 0.1 nm slit, shows only one emission line longward of 80 nm (O II, III, 83.5 nm blend); more would be expected using a longer exposure and narrower slit. Because the rocket altitude was rather low, the continuum is covered with absorption bands of atmospheric nitrogen. The Harvard photoelectric spectrum, because of greater dynamic range than the photographic, extends the Lyman continuum to approximately 70 nm; the absorption bands are absent because the altitude of the orbiting solar observatory was great enough to avoid all absorption effects. Below 50.4 nm the continuum of He I is intense in the photoelectric record, nearly swamping Si XII, 49.9 nm, whereas in the photographic spectrum the Si XII line is strong and the continuum weak because of the narrower slit. In OSO–VI, placed in orbit on 9 August 1969, Harvard has obtained spectra of this type, not just for the Sun's centre but also for a great many special regions, with 35″ × 35″ spatial resolution (L. Goldberg, unpublished). The spectral range of both the OSO–IV and VI instruments is limited to wavelengths less than 136 nm by the photocathode, and to wavelengths greater than 28 nm by the reduced sensitivity associated with normal-incidence optics.

Grazing-incidence spectroscopy

From 63 nm to shorter wavelengths is the range where grazing-incidence spectrographs become more powerful than normal-incidence. Photographic spectra have been obtained by N.R.L. (Austin *et al.* 1967; Widing & Sandlin 1968), Culham (Jones, Freeman & Wilson 1968), the U.S.S.R. (Zhitnik *et al.* 1967) and the Goddard Space Flight Center (Behring, Cohen & Feldman 1969).

Photoelectric grazing-incidence spectra have been recorded by the Air Force Cambridge Research Laboratories (A.F.C.R.L.) (Hinteregger & Hall 1969; Hinteregger 1965) from rockets on many occasions and from OSO–III; from OSO–I, III, and V by G.S.F.C. (Neupert *et al.* 1969). These grazing-incidence instruments until now have taken radiation from the entire Sun; spatial resolution could only be inferred from the time changes in the spectrum, resulting from solar rotation or a flare. By using a grazing-incidence Wolter lens to image the Sun on the

entrance slit, the G.S.F.C. grazing-incidence monochromator being constructed for OSO–H is expected to resolve 20″ spatially. Relative spectral intensities, in spite of much work, are still less certain than is desired for ionization theory calculations.

From 63 to 17.1 nm the spectrum is intense and rich, particularly so for wavelengths less than 37 nm; but from 17.1 to 14.8 nm it is weak, with few lines. About 500 solar lines have been distinguished from 63 to 14.8 nm; perhaps one-third have been identified. They are high chromospheric and coronal, with the greatest number coming from the transition region.

Shown in figure 3 is the range 18 to 14.8 nm where the spectrum changes from rich to poor. The A.F.C.R.L. photoelectric spectrum (Hinteregger & Hall 1969), is matched with an N.R.L. photographic spectrum (Tousey, Austin, Purcell & Widing 1965), both recorded when the Sun was quite active. (Counts per second are plotted logarithmically against wavelength.) The agreement is remarkably good; wavelength precision is greater for the photographic spectrum, but intensities are more accurately determined from the photoelectric spectrum. Photoelectrically recorded lines with signals below the 200 counts per second level were not detected in the photographic spectrum; it is probable that low-count peaks resulted largely from statistical noise, since at 40 counts per second a single data point received only three counts.

At the bottom of figure 3 is introduced the spectrum of the high temperature plasma produced by Zeta, as recorded by the Culham Laboratory (Fawcett *et al.* 1963). The story of the astonishing coincidence between the spectra of Zeta and the Sun, and the great contribution made by Culham to the identification of these lines is well known.

The least known section of the solar extreme u.v. is the short span 14.8 to about 11 nm. As yet, this has been covered only by A.F.C.R.L. (Hinteregger, Hall & Schweitzer 1964). Certainly some lines are present; but only a very few are above the noise level and their identifications are not certain.

Below about 11 nm the spectrum has been recorded quite thoroughly: photographic spectra by N.R.L. (Austin *et al.* 1967; Widing & Sandlin 1968), Culham (Jones *et al.* 1968), and the U.S.S.R. (Zhitnik *et al.* 1967; and photoelectric grazing-incidence spectra by A.F.C.R.L. (Manson 1967). The line count from 11 to 1.5 nm is approximately 200, of which about one-half have been identified. Figure 4 shows a short section of this range. A photographic spectrum obtained by N.R.L. is compared with a photoelectric spectrum of A.F.C.R.L., both recorded when the Sun was quiet. Also included is a microphotometer trace of the Zeta spectrum (Gabriel & Fawcett 1965). Again the agreement between the two solar spectra and the spectrum of the Zeta plasma is remarkable. In this range identification was made easier by the extensive laboratory spectroscopy of Edlén and others (Edlén 1964), and the situation seems to be fairly well in hand. The lines are high chromospheric, transition region, and coronal. Most of them are from transitions where the total quantum number changes, in contrast to the intense spectrum from 17.1 nm to longer wavelengths where the lines are mostly produced by screening transitions.

To photograph the spectrum below 3 nm becomes increasingly difficult. The Culham Laboratory has reached 1.5 nm (Jones *et al.* 1968; Gabriel & Jordan 1969), with a beautiful spectrum showing the ^1P and ^3P to ^1S lines of C v, N vi, and O vii, and for C v and O vii the forbidden lines also, ^3S to ^1S. The short wavelength record for photography is held by the U.S.S.R. (Zhitnik *et al.* 1967); owing to the occurrence of a flare during the rocket flight, lines were recorded to 0.95 nm. But the range below 2 or 3 nm is really the realm of the Bragg crystal spectrometer. Many soft X-ray lines have been discovered, especially during flares, a topic covered by W. M. Neupert (this volume, p. 143).

Summary of the observed extreme u.v. solar spectrum

As a summary of today's status of the observed extreme u.v. solar spectrum a rough count of the number of solar lines observed per nanometre is presented in figure 5 for the entire range to 3 nm. The sections over which the counts were made follow the discussion in the preceding paragraphs. Included for comparison is the region observed from the ground; the count is of Fraunhofer lines listed by Moore, Minnaert & Houtgast (1966). From 300 to 210 nm, the count is from the N.R.L. echelle spectra (Tousey, Purcell & Garrett 1967). To shorter wavelengths, the emission line counts are mainly from the N.R.L. and Culham photographic spectra, supplemented in various regions by lines detected in the various photoelectric spectra.

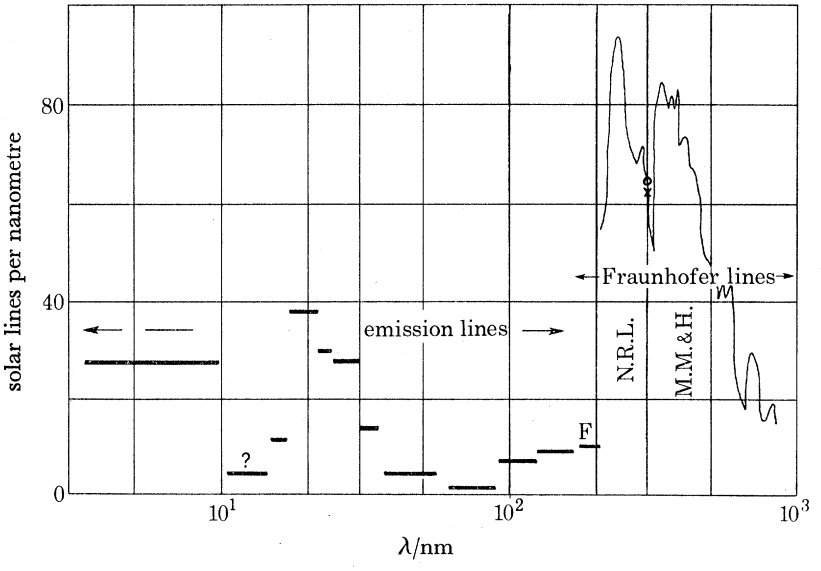

Figure 5. The status of the solar spectrum for $\lambda > 3$ nm, estimated by counting the number of observed lines per nanometre.

The number of Fraunhofer lines per nanometre increases sharply with decreasing wavelength despite the fact that the intensity of the continuum against which they are observed is decreasing rapidly. The principal reason is that the spectra of the abundant solar elements contain many more strong lines per nanometre as the wavelength is reduced and their resonance lines are approached. The great drop below 240 nm may be instrumental, but it is present also in the Culham echelle spectra reported in the accompanying paper by Boland *et al.*, p. 29. However, the discontinuity at 208.5 nm is at least partly an instrumental effect resulting from the sudden decrease in continuum intensity by a factor of 5; therefore Fraunhofer lines must be quite strong to be detected. The resolving power 10^5, already attained, seems to be nearly sufficient for separating most of the Fraunhofer lines. Gains will come, most probably, by increasing the signal to noise level of the spectrograph.

The emission line spectrum to shorter wavelengths presents a different situation from the Fraunhofer lines. The count is highly variable but generally low, running from about 1 to 40 lines per nanometre. In part, this reflects the speeds of spectrographs that are available for the different ranges, but it is also a result of changes in the character of the solar spectrum itself. The present limitation on the number of emission lines observed per nanometre is mainly a consequence of low instrumental speed and short exposure time, rather than spectral resolution and signal to noise

ratio. With longer exposures and instruments whose stray light background is low, it is probable that there would be observed at least as many emission lines per nanometre as there are Fraunhofer lines per nanometre at longer wavelengths.

For the emission line spectrum a resolution of about 10^4 may be sufficient because the high chromospheric and coronal lines will be some ten times broader than the weak photospheric lines, owing to the 100 times greater temperature of the region where they are formed. Nevertheless, 10^5 resolving power would be nice as a goal.

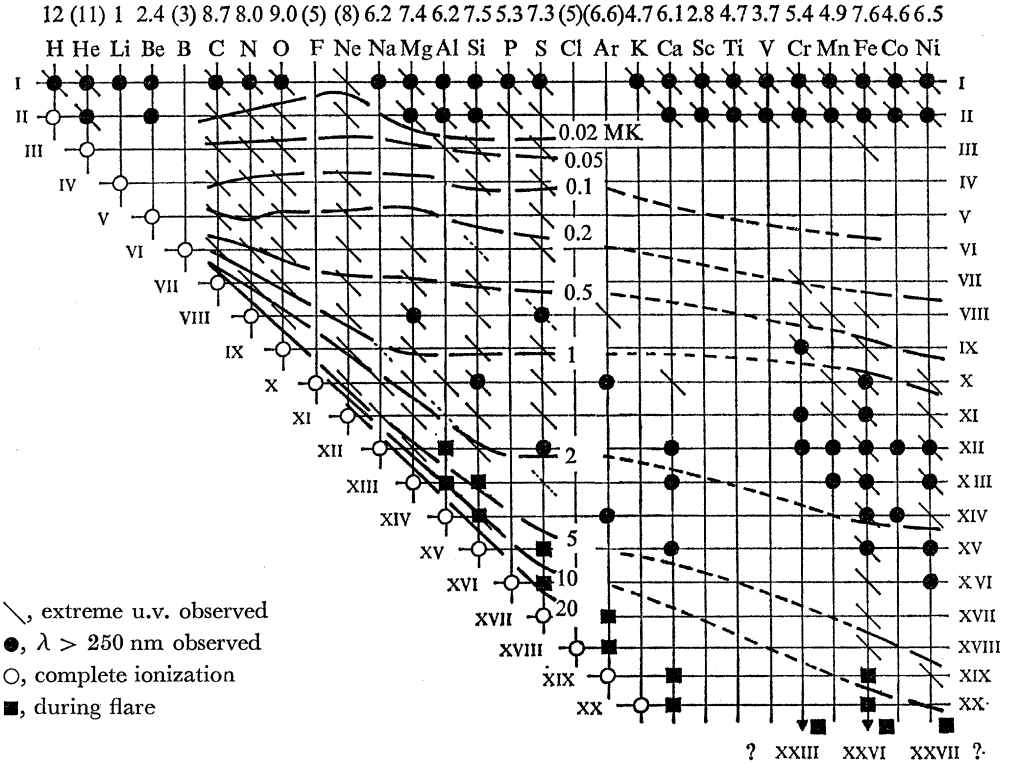

FIGURE 6. Ions detected in the sun by means of its extreme u.v. spectrum, and constant temperature curves, (from Jordan 1969), showing where the ion abundances maximize.

The overall conclusion is that an increase in spectroscopic sensitivity by at least one order of magnitude is needed to uncover the Sun's extreme u.v. spectrum to the extent that it is now known in the visible and near ultraviolet.

A summary of the atomic and ionic species found in the Sun from extreme u.v. space spectroscopy is presented in figure 6, a revision of earlier diagrams (Tousey 1968). New abundance values are shown for Fe and Ni (Unsöld, this volume, p. 23). The solid circles indicate species that have been recorded by ground-based observatories. Included are the forbidden coronal lines that are well-established, following the critical lists of Jefferies (1969), and of Edlén (1969). Species observed from space vehicles are shown by diagonal lines, dotted for a few identifications that are still in some doubt. The squares indicate ions detected with Bragg crystal spectrometers, mainly during flares. The inclusion of Cr XIII, Fe XXVI, and Ni XXVII with question marks is intended to indicate that many stages of ionization higher than XX have been observed during flares, but that

some of the identifications are still in doubt. More resolution, better wavelengths, and more laboratory and theoretical work are required to untangle the lines seen in flares and to decide to what extent non-thermal processes are involved in their excitation.

In order to show the regions of the Sun's atmosphere where the various ions occur, curves for the temperature at which each ion reaches maximum abundance relative to the other ions of the same elements are introduced into figure 6, making use of data from Jordan (1969). The intensities of the lines produced by the various ions depend not only on the abundance of the element and the relative abundance of the ion, but also on the solar model and the f value for the particular line. Although this is over-simplification, it does give some idea of the distribution of ionic species in the chromosphere and corona, and in active regions and flares.

All the ions of H, He, C, N and O have been observed, but many ions of elements of abundance less than 8 are missing. No extreme u.v. emission lines have been detected from ions of elements of abundance less than 6 with the exception of Cr and Mn; but their values of photospheric abundance may be low, as was true formerly of Fe and Ni.

Examining isoelectronic sequences, the H and He sequences are complete to Ca for elements of abundance greater than 6, and the Li and Na sequences are nearly so. The F and Ne sequences fall at the other extreme. In the F sequence nothing is certain between Ne II, 46.07, 46.24 nm, and Fe XVIII, 1.4 to 1.6 nm, except the forbidden coronal line of Ar X. The Ne sequence is completely empty between Ne I, 73.5 nm, which is very faint, and Fe XVII and Ni XIX in the X-ray range.

The distribution of ionic species with temperature can be seen from the constant temperature lines in figure 6. For temperatures less than 0.5×10^6 K no forbidden coronal lines have been detected; the highest stage ions are C V, O VI, Ne VI, Mg VI, Si VII, Cr VIII, Mn VIII, and Fe VIII. Extreme u.v. spectroheliograms observed for ions in this range are similar to Hα, and produce no coronal emission. Therefore this range is chromospheric.

From 0.5 to 2×10^6 K is the broad transition range from the chromosphere to the true corona. Many forbidden coronal lines are present. These extreme u.v. spectroheliograms are not like Hα; they change character with increasing temperature for the ions lying between these boundaries, thus confirming the transitional nature of this range. The greatest change takes place between Ne VII maximizing at just over 0.5×10^6 K, Mg IX at 1×10^6 K, and Mg X at nearly 2×10^6 K.

For temperatures from 2 to 5×10^6 K, the emission is from the quiet corona and from plages, as can be seen from extreme u.v. spectroheliograms and from the observed coronal lines. These include O VIII, Ne X, Mg XI, Al XII, Si XII, and Fe XV. Si XI and Fe XIV have much the same character.

For temperatures above 5×10^6 K the emission is principally from the hottest parts of centres of activity, and from flares. The ions involved include Na XI and Mg XII, both of which are enhanced in flares, and Al XIII, Si XIV, S XV, S XVI, Ar XVII, Ar XVIII, Ca XIX and Ca XX, which are hardly ever seen except in flares.

In the diagram of figure 6 there is no hint of an explanation of the curious absence of ions in the neon and fluorine isoelectronic sequences. To be sure, most of the expected species would be chromospheric and the chromosphere is thin from 0.1 to 0.2×10^6 K because of the steepness of the temperature rise; but in this region there are strong observed lines of ions of C, N, O and S, and even a line of Ne IV. Therefore it seems doubtful that the principal reason for the absence of the neon-like and fluorine-like ions is the steepness of the temperature distribution and thinness of the chromosphere, as Zirin has proposed (Zirin, Hall & Hinteregger 1963).

The reason for the absence of neon-like ions may simply be that the lines are difficult to excite.

PHILOSOPHICAL TRANSACTIONS OF THE ROYAL SOCIETY A MATHEMATICAL, PHYSICAL & ENGINEERING SCIENCES

The outer shell is closed and there can be no screening transitions; but screening transitions are the type that produce most of the strongest extreme u.v. lines. With a closed shell and a total quantum number jump required, a collision may be more likely to produce ionization than excitation. This reasoning, however, does not apply to the fluorine sequence, where screening transitions can exist and are strong in the laboratory. A calculation of collisional excitation probabilities is required.

Exceptions to the dearth of observed neon-like and fluorine-like ions are the strong lines of Fe XVII, Ni XIX and Fe XVIII in the X-ray range. The following simple qualitative explanation is proposed: An ion with a high value of positive charge, for example Fe XVII, will exert a strong coulomb attraction on an electron that happens to be on a near-collision course, thus increasing the probability of collision: Therefore the probability of collisional excitation will be much greater for ions with high values of charge than for low-stage ions in the early part of the same isoelectronic sequence.

Abundance determinations can be made from the intensities of lines excited during flares. For example, the X-ray lines of Ca XIX and XX are much stronger in the N.R.L. OSO–VI spectra than the corresponding lines of Ar XVII and Ar XVIII, although the cosmic abundance of Ar is four times greater than that of Ca (J. H. Meekins 1970, personal communication).

Extreme u.v. spectroheliograms

Spectroheliograms in the extreme u.v. have been recorded from OSO–II and OSO–V by N.R.L. (Tousey 1967), and from OSO–IV and OSO–VI by the Harvard College Observatory (Goldberg *et al.* 1968). The OSO spectroheliograms are extremely valuable because of the great time span covered, and in the case of the Harvard instrument because of their truly monochromatic character. However, the spatial resolution has not yet exceeded approximately 30″.

Photographic spectroheliographs flown in rockets by N.R.L. (Tousey 1967; Tousey, Sandlin & Purcell 1968), have produced monochromatic solar images with spatial resolution as great as a few seconds of arc. A slitless single-grating spectrograph is used, producing a spectrum of solar images which overlap. A thin aluminium filter interposed in front of the film eliminates long-wavelength stray light. Gratings of 2400 and 3600 lines per millimetre spacing and 1 m radius of curvature are used, producing images of 4.2 mm diameter, or 3.9 and 2.6 nm equivalent, respectively.

The spectroheliograms reproduced in figures 7 and 8, plate 5, were made using a 3600 lines per millimetre grating (Purcell & Tousey 1969). A spatial resolution of about 10″ was achieved except near the limb, where rocket precession induced image rotation caused it to be reduced. Figure 7 shows the Sun's appearance in the low chromospheric lines He I, 58.4 nm; He II, 30.4 nm (second-order image); O IV, 55.5 nm; and O V, 63.0 nm. Also present are the coronal lines Mg X, 61, 62.5 nm and Fe XV, 28.4 nm in second order. A long exposure covering shorter wavelengths is reproduced in figure 8; this shows He II, 30.4 nm in first order; the transition zone line Mg IX, 36.8 nm; the coronal lines Fe XV, 28.4 nm; Fe XVI, 33.5, 36.1 nm; and many images of fainter lines.

The chromospheric network is present in He I, He II, O IV and O V. It is blurred in O IV because this image is produced by 4 lines of O IV that span 0.2 nm. The presence of the network in the O V image shows that it extends to at least 0.2×10^6 K in the chromosphere. Just how much higher it may reach is not known. However a limit can be set, because in Ne VII, 46.5 nm, which maximizes

at 0.5×10^6 K, no network has been detected; this is the ion next higher than O v with which satisfactory spectroheliograms have been obtained.

A narrow limb-brightened ring, characteristic of optically thin lines, is present in the chromospheric and transition region lines. This ring is prominent in O v, Ne vii (not shown), and especially so in Mg ix. A ring is also present in He ii and probably in He i, but is very narrow and variable. For coronal lines the emission over the limb is strong but diffuse. It shows its presence first in Mg ix. In the He ii, 30.378 nm image there is intense emission over the limb, but the situation is complicated; one part is coronal, produced by Si xi, 30.331 nm, a line only 47 pm to the blue. The other part is from prominences which are intense in He ii and are absent in Si xi and all coronal lines.

The limb-brightened ring emission is destroyed wherever there is a prominence, for example, the great prominence in the He ii image in figure 8, located on the right and extending well above the centre line. Examination of this part of the O v, 63 nm image (figure 7) shows that emission of O v is greatly reduced or absent over the region where the prominence should be. This is a characteristic of almost every He ii prominence; it destroys the limb- brightened ring and may also reduce the nearby emission, in O v, Ne vii, and Mg ix. No doubt the same would be true for other lines if suitable images had been obtained. This effect suggests absorption by a cool gas, but these lines are too far removed from the Lyman continuum of H and the continuum of He i for absorption to be the cause. It seems probable that the prominence cools the entire solar atmosphere through which it extends, so that the concentration of higher-stage ions is reduced. Considered from another point of view, the prominence is associated with an upward bulge of the low chromosphere; this destroys the steep temperature rise in the chromosphere which is normally in the form of a thin spherical shell that produces the bright ring.

The intense coronal emission above the upper left limb (12° N, 90° E) is shown in more detail in figure 9, plate 6, for the blend of He ii and Si xi, Mg ix, and Fe xv. The He ii images were made with different exposure times. The Mg ix image is overlapped by other lines and the emission to the left of the dotted arc should be disregarded. The coronal emission in the He ii, 30.378 nm image really belongs to Si xi, 30.331 nm. This is clear from the fact that it appears to be floating above the limb, separated by a narrow black arc that is really the non-emissive Si xi photospheric limb. The structure present in the coronal emission itself is different in Mg ix, Si xi and Fe xv. The coronal emission is most structured in Mg ix, as is true also for the plages.

A plume is present in the He ii, 30.4 nm image, arising from the centre of the coronal emission. This plume appears to be a surge prominence. It was not detected in any other emission line, therefore it is believed to be associated with He ii, 30.4 nm, and not with the coronal Si xi image. It might have been recorded in Hα, had an image been obtained at the same time. It may be visible also in He i, 58.4 nm, but is extremely faint.

The best extreme u.v. spectroheliograms were obtained on 4 November 1969 by N.R.L. (Purcell & Tousey 1970), using a 2400 lines per millimetre grating whose radius of curvature was 2 m. This produced images of 9.5 mm diameter. The Aerobee rocket was launched during a flare that was classified as just barely of importance 2*N*. Figure 10 is a plot of the X-ray flux during this flare recorded by Solrad IX. By the time the rocket could be launched and had reached altitudes sufficient to record the extreme u.v. it was 7 min after the start of the flare and 2 min after the Hα maximum. At the beginning of the 4 min extreme u.v. exposure period the 0.8 to 2 nm flux had decreased from maximum by a factor of 2, and at the end it had decreased by another factor of 2. The decrease in the shorter wavelength X-ray ranges was even greater.

PHILOSOPHICAL TRANSACTIONS OF THE ROYAL SOCIETY A MATHEMATICAL, PHYSICAL & ENGINEERING SCIENCES

A section of the 4 November 1969 spectroheliogram is reproduced in figure 11, plate 6. This shows images in He II, 30.4 nm; Fe XV, 28.4 nm that overlaps halfway; Fe XVI, 33.5 nm, and small parts of Fe XVI, 36.1 nm, and Mg IX, 36.8 nm. The instrument was prevented from rolling and held stable in yaw and pitch to 3 or 4″ with the Sparcs system, developed by the Ames Research Center. The resolution at the centre of the He II image is about 5″ and for shorter exposures

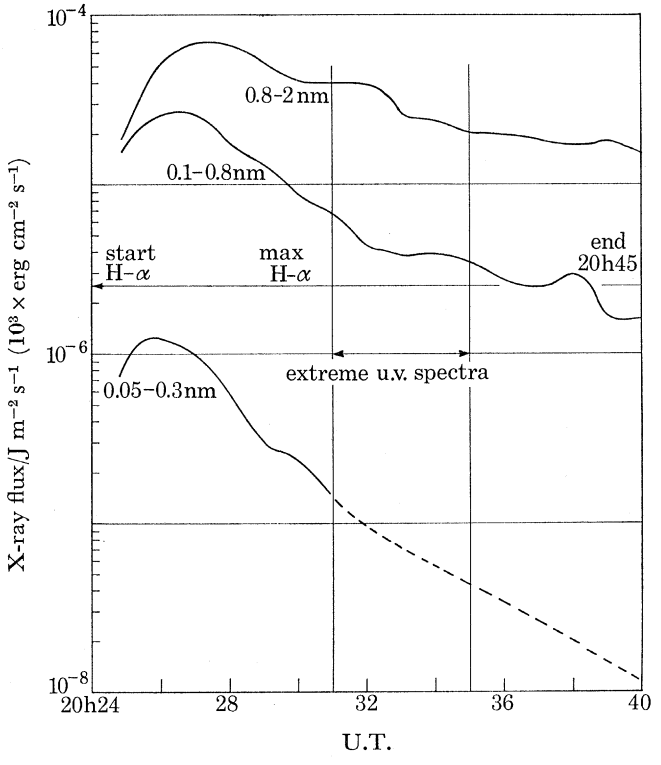

FIGURE 10. A plot of the X-ray flux measured by Solrad-9 for the importance 2N flare whose form and spectrum were photographed with the N.R.L. spectroheliograph on 4 November 1969 between 20 h 31 and 20 h 35 U.T.

reached 3″. The chromospheric network is extremely prominent. On the original, many spicules or clumps of spicules can be resolved. The great butterfly-like plage in the lower left quadrant is one of the most conspicuous features, changing appearance from line to line, from a highly structured series of intense bright filaments and points in chromospheric lines, to a diffuse pair of clouds still retaining some structure in the coronal lines. Because of overexposure the tiny flare nucleus cannot be seen in the He II, 30.4 nm image in figure 11, plate 6; only the plage in which it appeared and a loop prominence are visible.

The images of the flare itself are shown in figure 12, plate 7, for a series of lines that require greater and greater temperatures for formation. The Hα image is poor; a search is continuing to find a better image. In He I and He II the flare is a parallelogram with the bright nucleus showing at one end, and a bright thread-like filament extending from the nucleus to the upper end of the flare. This can be seen much better in He II, 25.6 nm (figure 11). The appearance is similar in O IV, but is confused by the presence of the four lines in this multiplet. O V and Ne VII show the same structure but with differences in the bright filament, and in the bright points below the nucleus. In Ne VII the first signs of coronal emission are seen, as might be expected because some emission from this ion extends to coronal temperatures, although it maximizes at about 0.5×10^6 K.

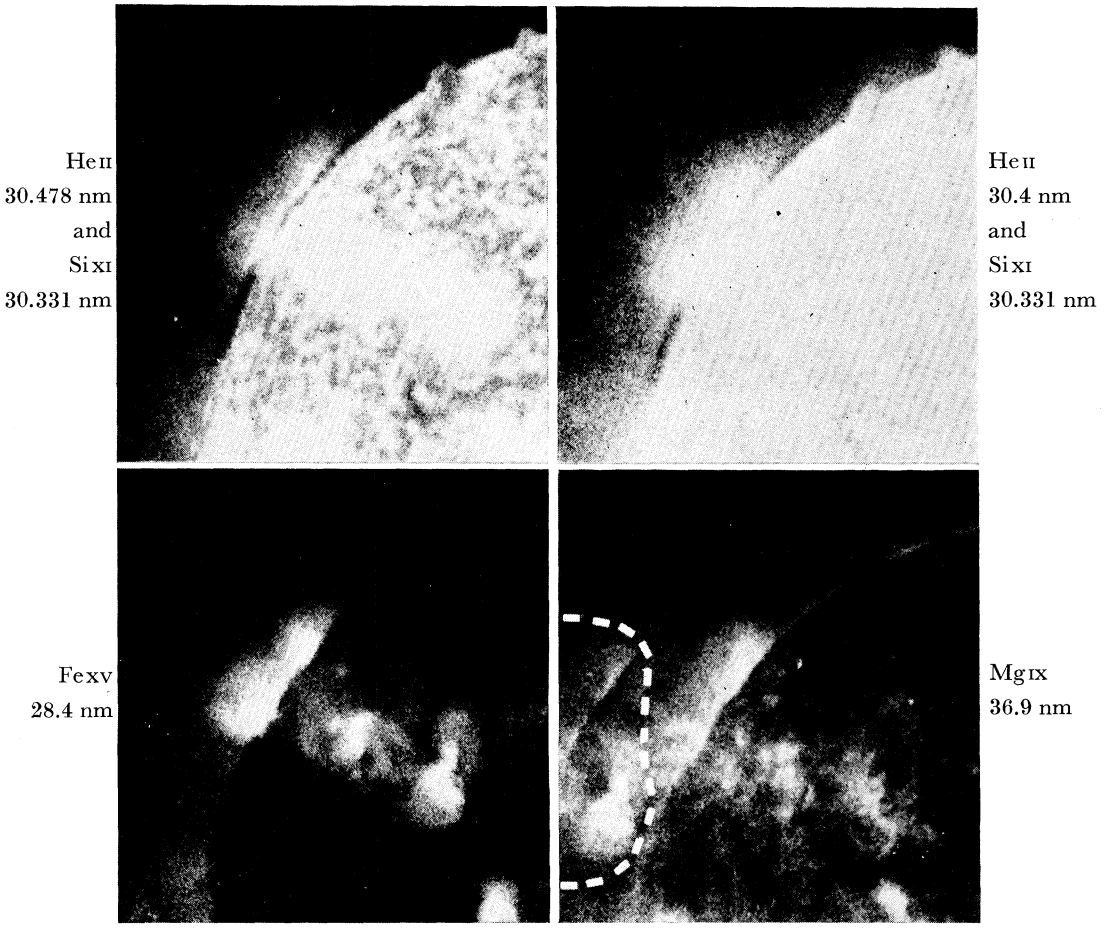

FIGURE 9. Magnified portions of the 22 September 1968 N.R.L. spectroheliograms. The blend of HeII and SiXI is well resolved. The coronal emission is different in structure in MgIX, SiXI, and FeXV. The plume from its centre is believed to be a surge prominence in HeII.

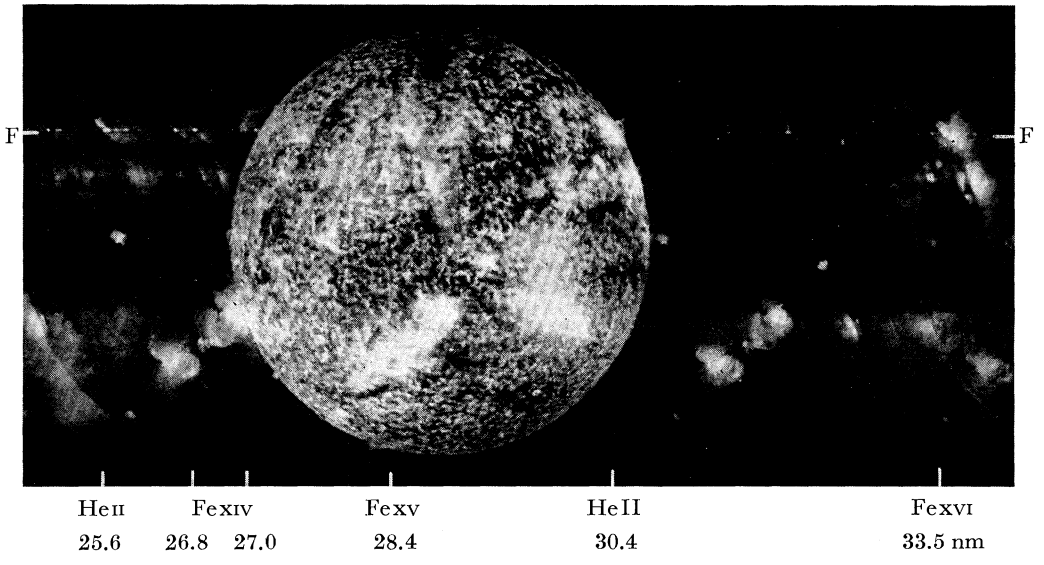

FIGURE 11. A portion of a spectroheliogram made by N.R.L. on 4 November 1969 in the declining phase of an importance 2*N* flare, located at 78° E, 5° N, heliocentric. The flare nucleus measured 6″ in diameter; in chromospheric lines it was accompanied by a bright filament and enhancement in the plage: in coronal lines it enhanced the diffuse emission above the limb.

(*Facing p.* 68)

PHILOSOPHICAL TRANSACTIONS OF THE ROYAL SOCIETY A MATHEMATICAL, PHYSICAL & ENGINEERING SCIENCES

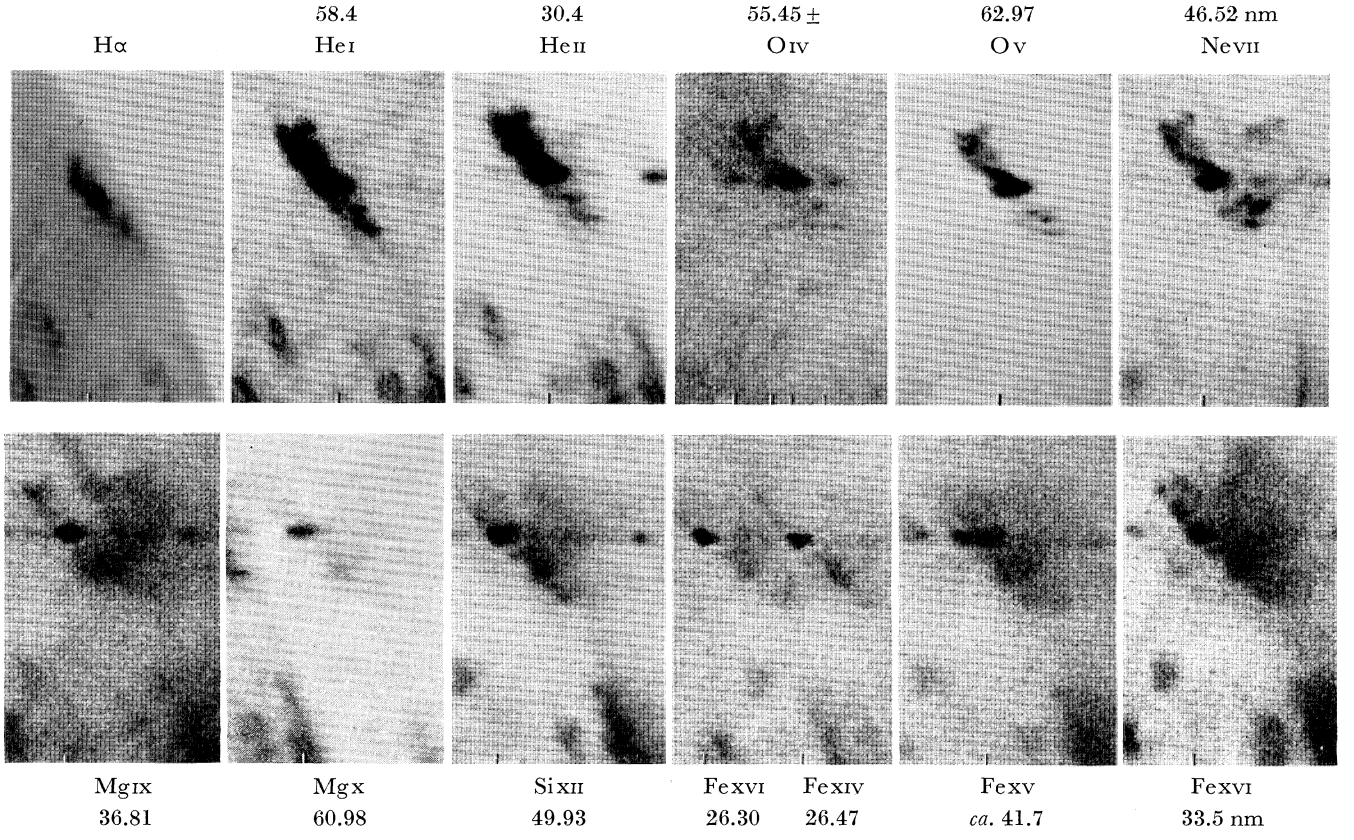

FIGURE 12. Spectral images of the importance 2*N* flare, photographed by N.R.L. at 20 h 34 U.T. on 4 November 1969. The Hα image is from Essa, Boulder, Colorado. The upper images are from chromospheric lines, the lower from coronal. Ne VII and Mg IX show the appearance of the flare in the transition region.

The great change takes place beginning with Mg IX, maximizing at 1×10^6 K. In this image there is principally the hot bright nucleus, surrounded by a great deal of coronal emission; the detailed emission in the plage is reduced or diffused. Mg X is similar but the exposure is much weaker, hence the coronal emission is not as prominent. Si XII, a 2×10^6 K ion, continues the trend, which can be followed to Fe XVI, at 3×10^6 K. There the nucleus is still small and intense and in the same position; the coronal cloud surrounding it has increased in intensity; the bright filament is replaced by spotty diffuse emission.

In size the region enhanced during the flare in low chromospheric lines measured 6 square degrees, apparent, whereas the Hα flare was reported as 2.1 square degrees, apparent, at maximum. But in the high chromospheric and coronal lines, except for the diffuse coronal enhancement, the flare was just a nucleus measuring about 6″ in diameter or approximately 0.1 square degrees, apparent, after making appropriate corrections for pointing jitter and instrument profile.

In the He II, 30.4 nm image of figure 12, which is in second order, Doppler wings are present. These are the faint ghost-like images extending to both sides of the flare nucleus. The maximum displacement is ± 45 pm, indicating an expansion velocity of about 450 km s^{-1} in the line of sight, which was about 78° to the Sun's normal. This suggests as model of the flare nucleus, at a time well after maximum, a rapidly expanding and cooling plasma sphere. That the Doppler wings were not detected for other lines can be explained by their lesser intensity.

It is obvious that much could be learned about flares if many more images of this type were obtained and if the spatial resolution were somewhat improved. What is needed to accomplish this is a well-stabilized solid propellant rocket that can be held ready to launch at a moment's notice, a range without restrictions, and an active Sun.

I wish to thank my colleagues, G. E. Brueckner, J. D. Purcell and K. G. Widing, for their advice and assistance in the preparation of this paper.

References (Tousey)

Austin, W. E., Purcell, J. D., Snider, C. B., Tousey, R. & Widing, K. G. 1967 *Space research VII* (ed. R. L. Smith-Rose), pp. 1252–1261. Amsterdam: North Holland.
Behring, W. E., Cohen, L. & Feldman, U. 1969 *Bull. Am. astr. Soc.* **1**, 272–273.
Brueckner, G. E., Bartoe, J-D. F., Nicolas, K. R. & Tousey, R. 1970 *Nature, Lond.* **226**, 1132.
Burton, W. M., Ridgeley, A. & Wilson, R. 1967 *Mon. Not. R. astr. Soc.* **135**, 207–223.
Edlén, B. 1964 *Handb. Phys.* **27**, 80–221.
Edlén, B. 1969 *Solar Phys.* **9**, 439–445.
Fawcett, B. C., Gabriel, A. H., Griffin, W. G., Jones, B. B. & Wilson, R. 1963 *Nature, Lond.* **200**, 1303.
Gabriel, A. H. & Fawcett, B. C. 1965 *Nature, Lond.* **206**, 808.
Gabriel, A. H. & Jordan, C. 1969 *Nature, Lond.* **221**, 947.
Gabriel, A. H. & Jordan, C. 1969 *Mon. Not. R. astr. Soc.* **145**, 241.
Goldberg, L., Noyes, R. W., Parkinson, W. H., Reeves, E. M. & Withbroe, G. L. 1968 *Science, N.Y.* **162**, 95.
Hinteregger, H. E., Hall, L. A. & Schweitzer, W. 1964 *Astrophys. J.* **140**, 319–327.
Hinteregger, H. E. 1965 *The solar spectrum* (ed. C. de Jager), pp. 179–205. Dordrecht: D. Reidel.
Hinteregger, H. E. & Hall, L. A. 1969 *Solar Phys.* **6**, 175–182.
Jefferies, J. T. 1969 *Mém. Soc. Roy. Sci. Liège* (5) **16**, 213.
Jones, B. B., Freeman, F. F. & Wilson, R. 1968 *Nature, Lond.* **219**, 252.
Jordan, C. 1969 *Mon. Not. R. astr. Soc.* **142**, 501.
Lindsay, J. C. 1964 *Planet. Space Sci.* **12**, 379.
Manson, J. E. 1967 *Astrophys. J.* **147**, 703–710.
Moore, C. E., Minnaert, M. G. J. & Houtgast, J. 1966 *The solar spectrum* 2935 Å *to* 877 Å, N.B.S. Monograph 61 (U.S. Government Printing Office, Washington, D.C.).
Neupert, W. M., White, W. A., Gates, W. J., Swartz, M. & Young, R. M. 1969 *Solar Phys.* **6**, 183–192.
Parkinson, W. H. & Reeves, E. M. 1969 *Solar Phys.* **10**, 342–347.

PHILOSOPHICAL TRANSACTIONS OF THE ROYAL SOCIETY A MATHEMATICAL, PHYSICAL & ENGINEERING SCIENCES

Purcell, J. D. & Tousey, R. 1969 *Bull. Am. ast. Soc.* **1** (no. 3) 290.
Sandlin, G. D. & Widing, K. G. 1967 *Astrophys. J.* **149**, L129.
Speer, R. J. *et al.* 1970 *Nature, Lond.* **226**, 249.
Tousey, R., Purcell, J. D., Austin, W. E., Garrett, D. L. & Widing, K. G. 1964 *Space research IV* (ed. P. Muller), pp. 703–718. Amsterdam: North-Holland.
Tousey, R., Austin, W. E., Purcell, J. D. & Widing, K. G. 1965 *Ann. d'Astrophys.* **28**, 755–773.
Tousey, R. 1967 *Astrophys. J.* **149**, 239–252.
Tousey, R., Purcell, J. D. & Garrett, D. L. 1967 *Appl. Opt.* **6**, 365–372.
Tousey, R. 1968 *Beam-foil spectroscopy* (ed. S. Bashkin), vol. II, pp. 486–524. New York: Gordon & Breech.
Tousey, R., Sandlin, G. D. & Purcell, J. D. 1968 *Structure and development of solar active regions* (ed. K. O. Kiepenheur), pp. 411–419. Dordrecht: Reidel.
Widing, K. G. & Sandlin, G. D. 1968 *Astrophys. J.* **152**, 545–556.
Widing, K. G., Purcell, J. D. & Sandlin, G. D. 1970 *Solar Phys.* **12**, 52–62.
Zhitnik, I. A., Krutov, V. V., Malyavkin, L. P., Mandel'shtam, S. L. & Cheremukhin, G. S. 1967 *Kosmicheskie Issledovanya* **5**, 276.
Zirin, H., Hall, L. A. & Hinteregger, H. E. 1963 *Space research III* (ed. W. Priester), pp. 760–771. Amsterdam: North-Holland.

PHILOSOPHICAL TRANSACTIONS OF THE ROYAL SOCIETY A MATHEMATICAL, PHYSICAL & ENGINEERING SCIENCES

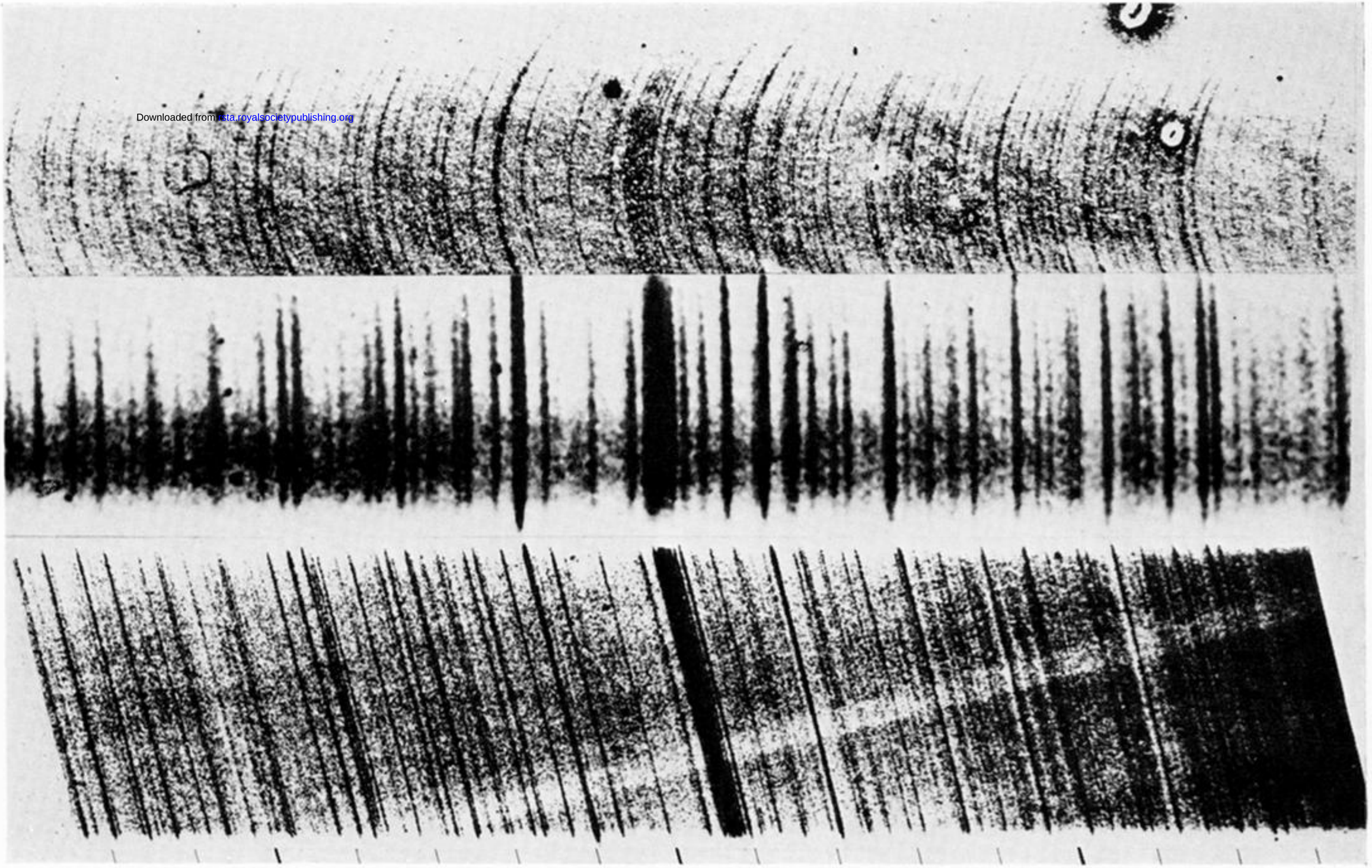

FIGURE 1. Solar spectra over a range that includes radiation from the temperature minimum and the chromosphere, with some contribution from the photosphere and the inner corona. At the top is a total eclipse flash spectrum obtained on 7 March 1970 by N.R.L. In the centre is the Culham 10″ off-limb spectrum of 9 April 1965. The bottom shows the N.R.L. double-dispersion spectrum of 1 February 1966, having a spatial resolution of about 10″.

PHILOSOPHICAL TRANSACTIONS OF THE ROYAL SOCIETY A MATHEMATICAL, PHYSICAL & ENGINEERING SCIENCES

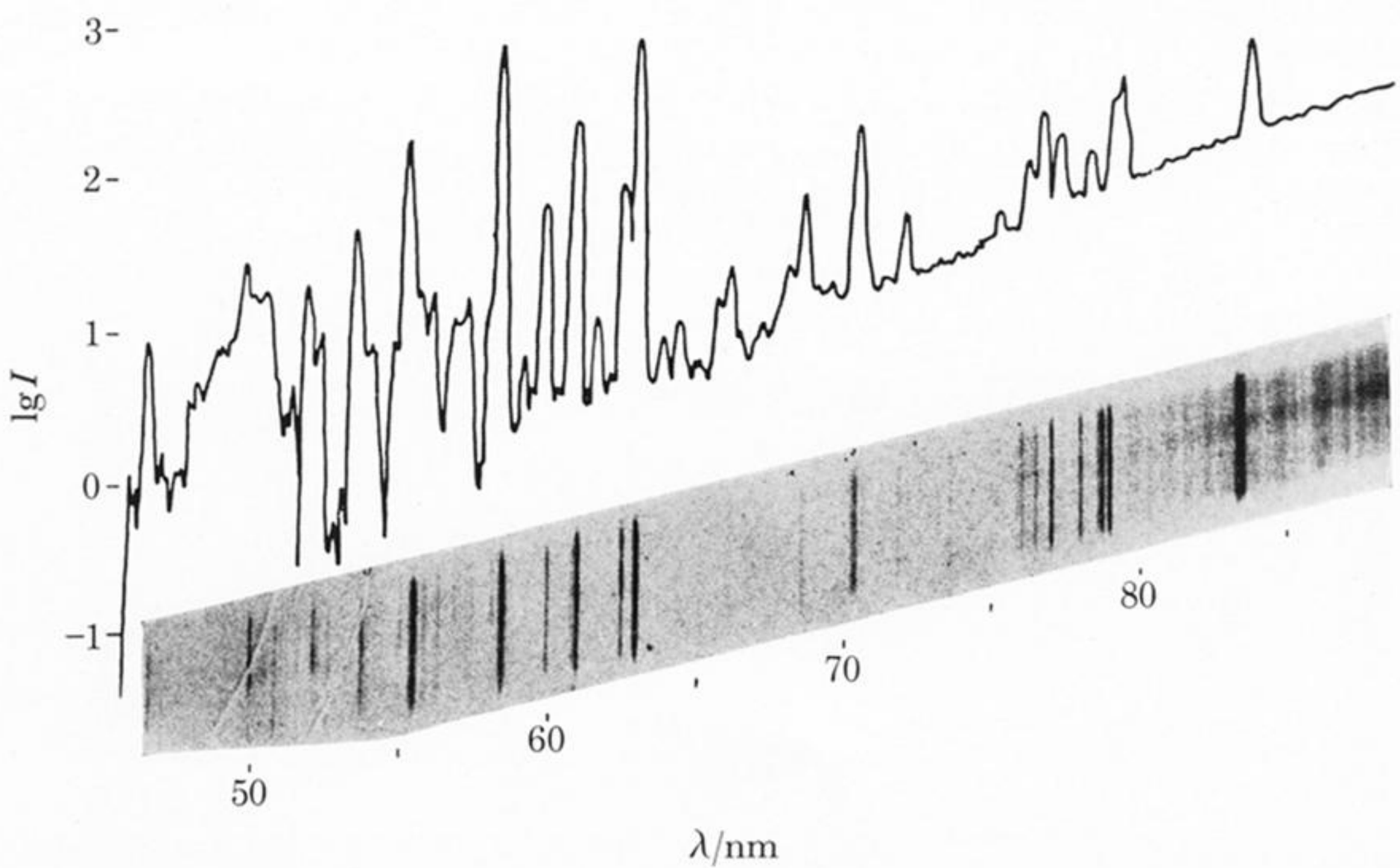

FIGURE 2. The N.R.L. double-dispersion stigmatic spectrum made on 27 July 1966 when the Sun was active, and an OSO–IV spectral scan of a 1′ × 1′ region at the centre of the disk, recorded by the Harvard College Observatory.

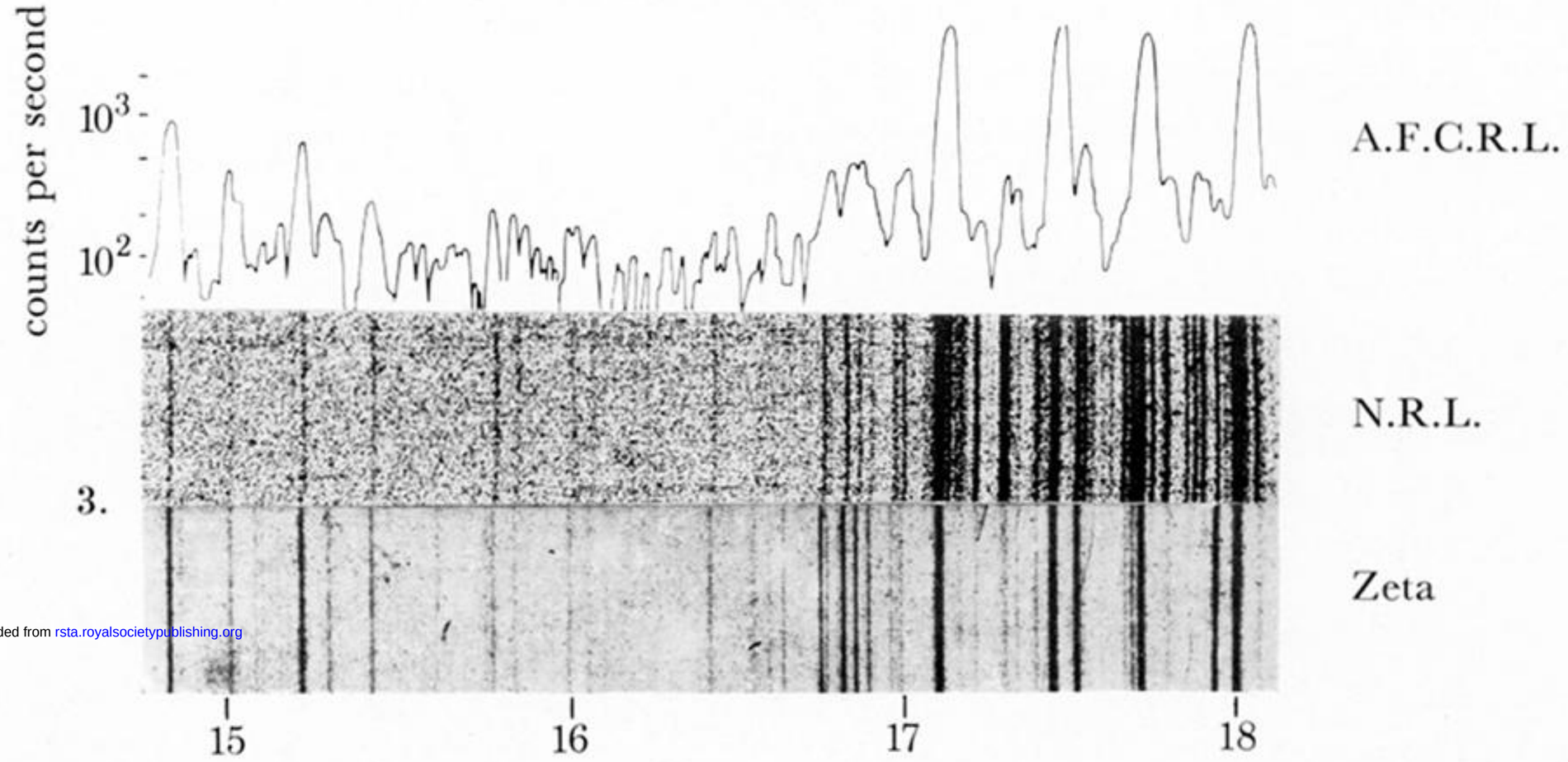

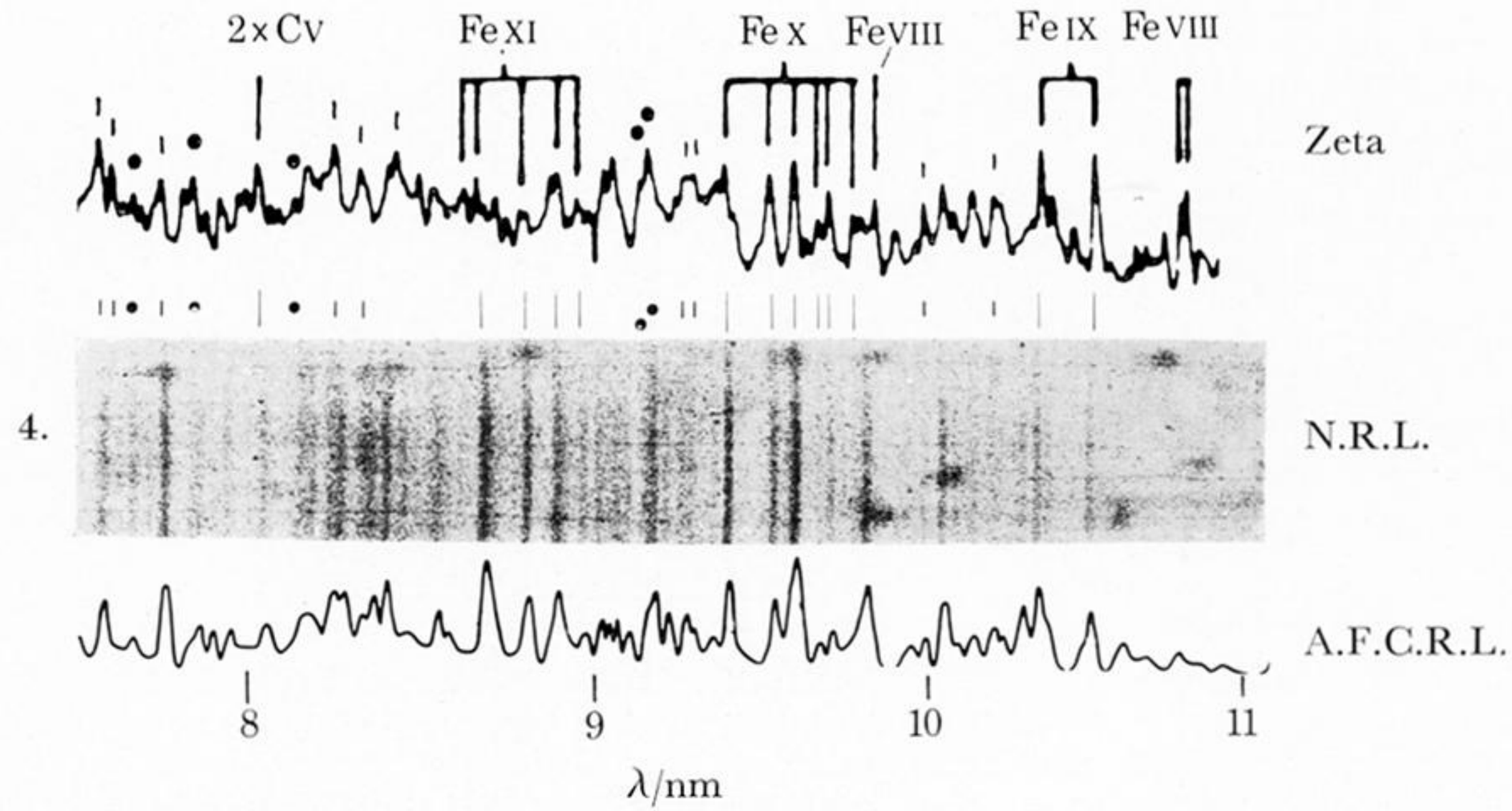

FIGURE 3. The N.R.L. spectrum of 20 September 1963 matched to the A.F.C.R.L. spectrum of 2 May 1963 and the spectrum obtained by the Culham Laboratory from the high temperature plasma produced by the Zeta discharge at Harwell.

FIGURE 4. The Sun's soft X-ray spectrum; photographed by N.R.L., scanned photoelectrically by A.F.C.R.L., and matched to a microphotometer trace of a photographic spectrum of the Zeta discharge, made by the Culham Laboratory.

55.5 58.4 30.4 63 nm

O IV He I He II(2) O V

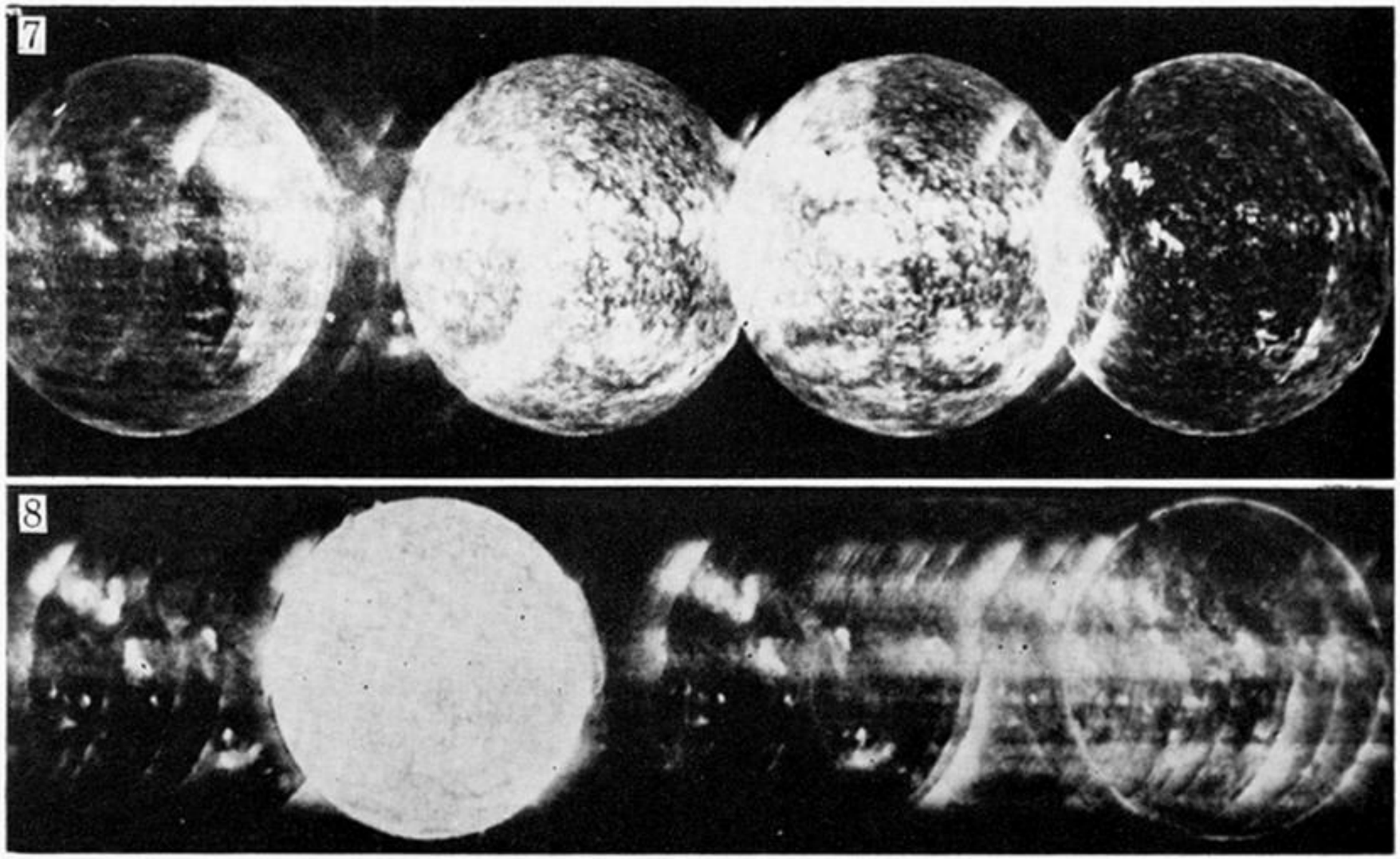

Fe XV He II (Fe XVI) Mg IX

28.4 30.4 (33.5 36.1) 36.8 nm

FIGURE 7. A spectroheliogram made by N.R.L. on 22 September 1968 with a 3600 line/mm 1 m radius objective-type grating spectrograph. The principal images are from the indicated chromospheric lines. Also easily seen are Fe XV, 28.4 nm in second order, and Mg X, 61, 62.5 nm.

FIGURE 8. A long exposure spectroheliogram made by N.R.L. on 22 September 1968 using a 3600 line/mm, 1 m radius objective-type grating spectrograph. The Si XI, 30.331 nm image is resolved from the He II, 30.378 nm image. A great prominence is present in He II on the right, extending above the centre line.

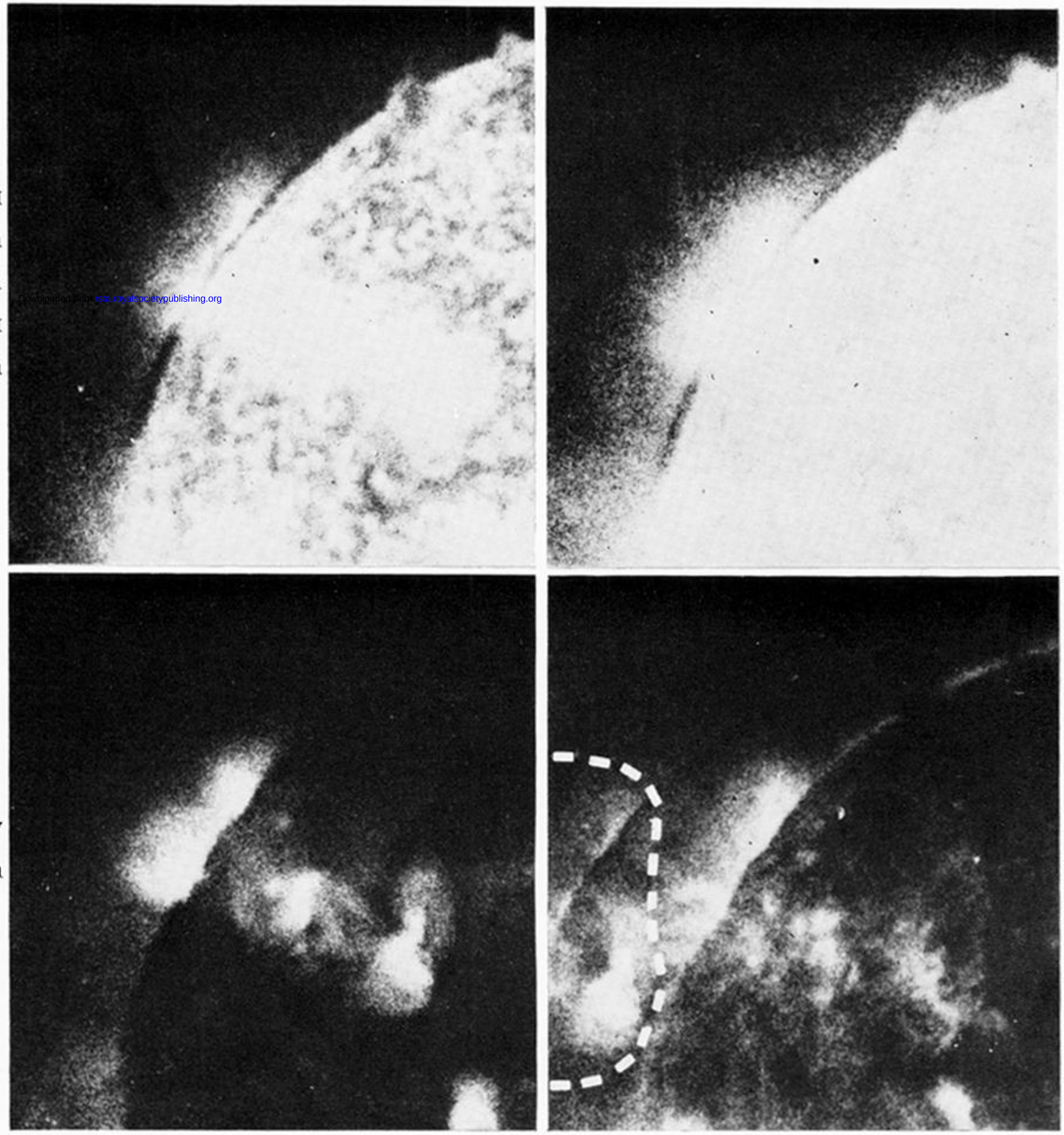

FIGURE 9. Magnified portions of the 22 September 1968 N.R.L. spectroheliograms. The blend of HeII and SiXI is well resolved. The coronal emission is different in structure in MgIX, SiXI, and FeXV. The plume from its centre is believed to be a surge prominence in HeII.

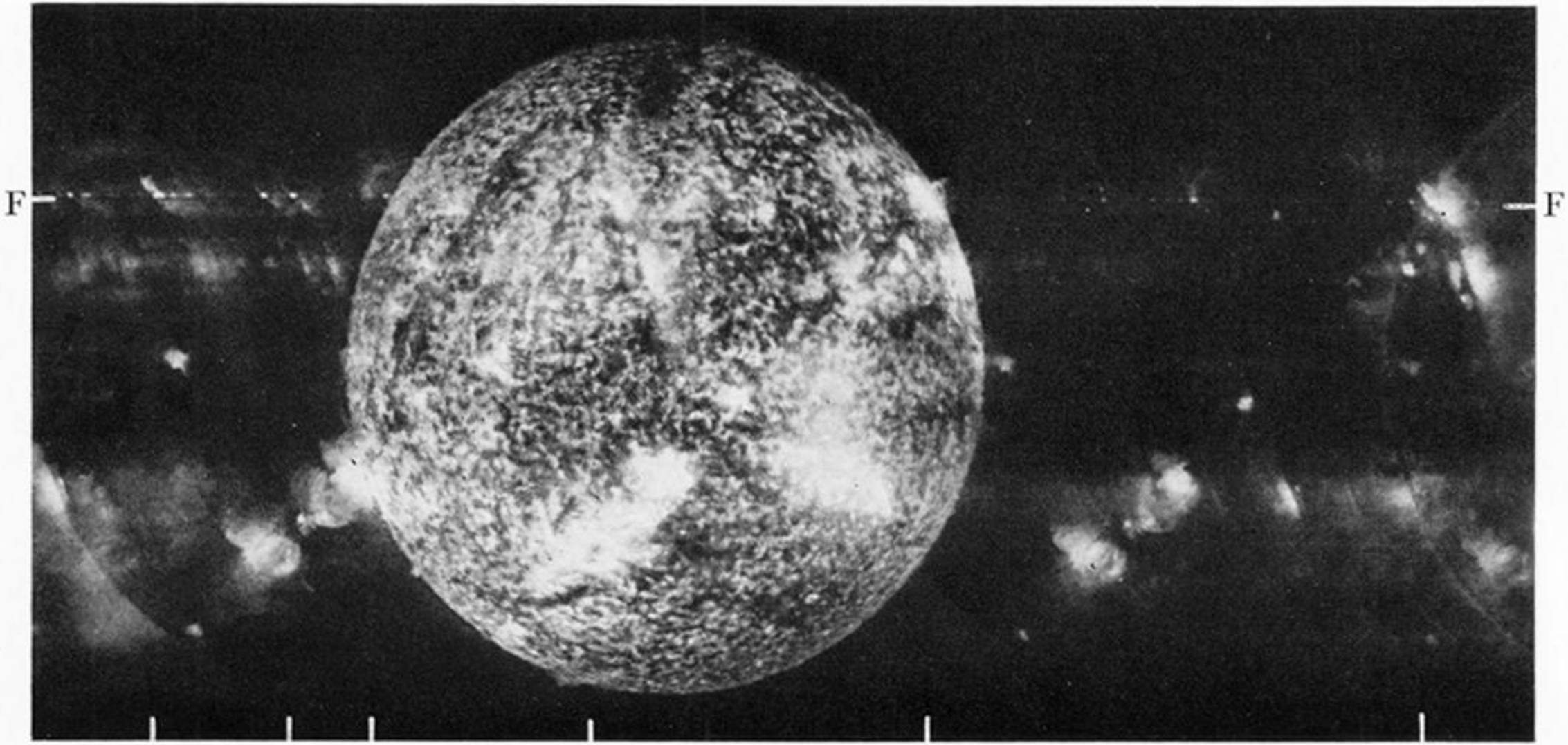

FIGURE 11. A portion of a spectroheliogram made by N.R.L. on 4 November 1969 in the declining phase of an importance 2*N* flare, located at 78° E, 5° N, heliocentric. The flare nucleus measured 6″ in diameter; in chromospheric lines it was accompanied by a bright filament and enhancement in the plage: in coronal lines it enhanced the diffuse emission above the limb.

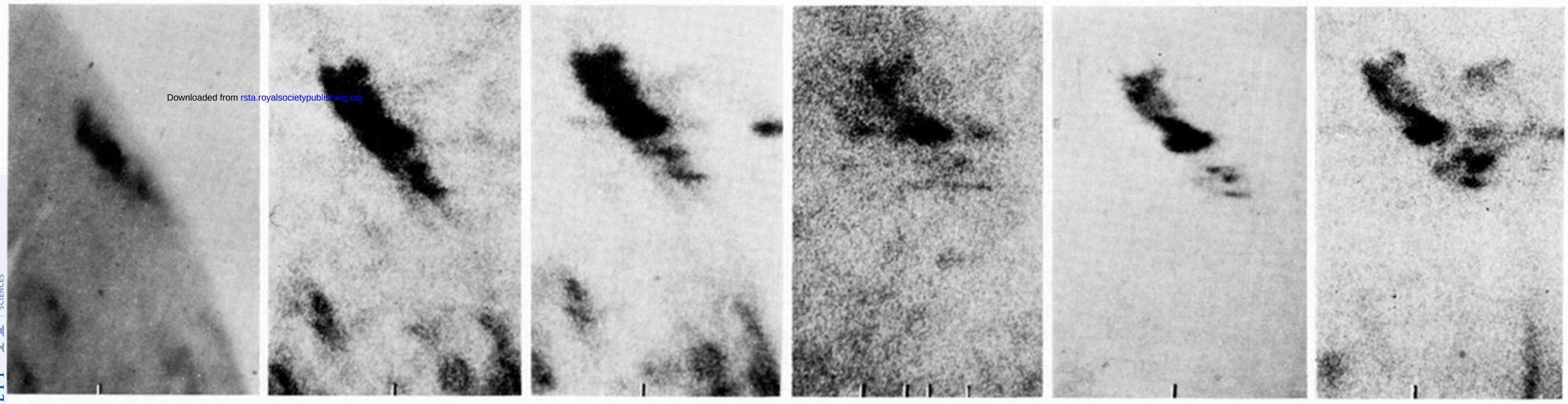

FIGURE 12. Spectral images of the importance 2*N* flare, photographed by N.R.L. at 20 h 34 U.T. on 4 November 1969. The Hα image is from Essa, Boulder, Colorado. The upper images are from chromospheric lines, the lower from coronal. NeVII and MgIX show the appearance of the flare in the transition region.